January 2018

Electrophysiology Of The Thalamus During Focal Limbic Seizures

William Angus Biche

Electrophysiology of the thalamus during focal limbic seizures

A Thesis Submitted to the

Yale University School of Medicine

in Partial Fulfilment of the Requirements for the

Degree of Doctor of Medicine

By

William Angus Biché

2018

Abstract

Temporal lobe epilepsy remains a common and complex clinical entity whose underlying disease pathology is incompletely understood. While many structures been identified in contributing to these seizures, particular note should be given to the thalamus. Previous studies with imaging techniques and neurostimulation have suggested certain thalamic nuclei of interest, but their precise activity during seizures has yet to be elucidated. The goal of this study was to perform population and single neuron recordings of several different thalamic nuclei during temporal lobe seizures, namely, the anterior (ANT), centrolateral (CL) and ventral posteriomedial (VPM). We performed these studies in an established rat model of temporal lobe epilepsy. We found that multiunit activity (MUA) increased during seizures in ANT and VPM, and decreased in CL. Additionally, single unit juxtacellular recordings showed a decreased firing rate and a switch to increased burst firing in CL. Finally, analysis of MUA in VPM showed a significant increase in spindles during seizures. These results reinforce our hypothesis that different thalamic nuclei have different roles in temporal lobe epilepsy, and generally support their previously hypothesized physiologic and pathologic functions. As a limbic nucleus, ANT participates in seizure propagation. CL, on the other hand, is a component of arousal circuitry and likely participates in decreased consciousness during seizures. Lastly, the increased spindle activity in VPM is also seen in sleep or light anesthesia, and may contribute to cortical dysfunction.

Acknowledgements

This study was initially published under the title “Seizures and Sleep in the Thalamus: Focal Limbic Seizures Show Divergent Activity Patterns in Different Thalamic Nuclei” in the November 2017 issue of the Journal of Neuroscience. It was authored by Li Feng, Joshua Motelow, Chanthia Ma, myself, Cian McCafferty, Nicholas Smith, Mengran Liu, Qiong Zhan, Ruonan Jia, Bo Xiao, Alvaro Duque, and Hal Blumenfeld. I would like to especially thank Li Feng for her friendship and support in this project, as well as Hal Blumenfeld for his ongoing mentorship.

Table of Contents

Statement of Purpose

Previous work in rodent models of focal limbic epilepsy have suggested the variable roles of different thalamic nuclei in the disease. While some are involved in propagation of seizures to the cortex, others have been implicated in loss of consciousness. It is our aim to record precise measurements of neuronal activity in several targeted thalamic nuclei to better characterize their individual roles in focal limbic epilepsy. We hypothesize that different thalamic nuclei will show different behavior during seizures based on previous understanding of their physiologic roles.

Introduction

Epilepsy is an unfortunately common disease entity that can cause significant morbidity and mortality amongst its victims (1). While epilepsy varies significantly in its clinical presentation, from mild sensory predominant focal seizures, to the more severe generalized seizures that leave patients unconscious and pose significant impact to their quality of life. These latter patients may be unable to hold a job, drive, or effectively care for themselves, if their seizures are uncontrolled by medical therapy. While advances in pharmacology have made seizure treatment more effective, further characterizing the pathophysiology of epilepsy may reveal new treatment paradigms and reduce disease burden.

Temporal lobe epilepsy is a subtype of epilepsy characterized by an epileptogenic focus within the temporal lobe, and is the most common subtype in adults and adolescents. Clinically, it usually manifests with an aura, typically remembered, that preceeds the seizure. These auras are occasionally smells or tastes, but more frequently are less tangible; sensations of déjà vu or falling are common. The seizures themselves are typically complex partial, with brief loss of consciousness, and, in some patients, full generalization (2). For those with focal limbic seizures, loss of consciousness has been ascribed to interruptions in key subcortical arousal systems (3, 4).

While many structures have been implicated in seizure pathophysiology and propagation, of particular note for limbic seizures is the thalamus. Critically involved in sensory inputs and many other neurocognitive processes, certain thalamic nuclei also serve as a processing center for information from the limbic system before transmission to the cortex. This pathway can be significant in propagation of focal (and particularly temporal lobe) seizures. Certain thalamic nuclei such as the anterior nucleus (ANT), have well defined roles in the limbic system and have long been suggested as critical to seizure propagation (5). In patients with focal limbic seizures, morphometric MRI shows ANT volume loss correlating with volume loss in both the mesial temporal cortex and hippocampus (6).

Impairment of thalamic function can also play a role in the impaired consciousness seen in focal limbic seizures. More recent work using high field blood-oxygen-level dependent (BOLD) fMRI has demonstrated suppression in the intralaminar thalamus during limbic seizures, which resolved postictally (7). The same study was able to correlate this suppression with a concurrent decrease in choline in the same structure, suggesting a role for this region in consciousness circuits. While these data are exciting, more direct measurement of thalamic activity is needed. BOLD fMRI data can be misleading as to base neuronal activity. While an increase in CBF has been correlated with increased neuronal activity in the thalamus, contrary findings have been noted in the hippocampus and striatum (8, 9). In addition to confirming the

aforementioned BOLD data, direct measurement of neuronal activity can also assess firing rate and pattern, rather than simply an increase or decrease in overall activity.

The present study focuses on that goal: more precisely measuring the electrophysiological changes in the thalamic structures during seizures. For analyzing activity of these structures we measure their multiunit activity (MUA) and single unit activity (SUA). MUA is a measurement of the spiking activity of a population of neurons and is useful for assessing the temporal response of brain structures to different stimuli. SUA, on the other hand, looks at single neurons and can elicit information on firing rates and patterns.

In this study, we present findings of an increase in ictal MUA in anterior thalamic nucleus (ANT) and ventral posteriomedial nucleus (VPM), and a decrease in ictal MUA in centrolateral (CL). These suggest varying roles for these different nuclei in focal seizures. For ANT, this could support previous theories of a role as a junction for seizure propagation. For CL, this could support previous findings as an important nucleus for arousal. Additionally, our measurements of SUA indicate a markedly decreased rate of fire amongst individual neurons in CL, coupled with an ictal shift towards burst firing. This firing method has been observed in other states of decreased consciousness, such as sleep and anesthesia (10). These last findings suggest a role in loss of consciousness for CL. Finally, we also examine the prevalence of spindle patterns of neuron firing in VPM, and report a significant increase during seizures. As spindles are classically seen in

states of decreased arousal (e.g. sleep and light anesthesia), this finding suggests a shared etiology of impaired consciousness and an interplay between the thalamus and other subcortical structures in arousal.

Materials and Methods

This project was the result of a team effort, with members at all stages of training, from undergraduates to postdocs. Different team members were responsible for different components. Li Feng and I performed the electrode implantation surgeries and electrophysiological data acquisition. Other components, including histology, were accomplished by other team members.

Animals

The Yale University Institutional Animal Care and Use Committee approved all procedural protocols. 38 adult Sprague-Dawley rats weighing 180-280 grams (Charles River Laboratories) were used for experiments. Previous studies of these rodents with temporal lobe epilepsy have demonstrated greater success rate in female rodents (11, 12), and so all experiments were conducted in females. 30 of these rodents were used in measurements of MUA in thalamic nuclei, and eight were used in juxtacellular SUA recordings from CL.

Surgery and electrode implantation

All animals were first deeply anesthetized with 90 mg/kg ketamine (Henry Schein Animal Health, Ashburn, VA) and 15 mg/kg xylazine (AnaSed; Llyod Laboratories,

Quezon City, Philippines) injected intramuscularly. Responsiveness to pain was checked every 15 minutes by toe pinch, and animals were kept under deep anesthesia during electrode implantation. Animals were kept warm by use of a heating pad set to 37C. In preparation for electrode placement, burr holes were placed stereotactically above the locations of electrode placement. All coordinates are reported in reference to bregma (13). A tungsten monopolar microelectrode (UEWMGGSEDNNM; FHC) with impedance of 3 - 4 MΩ was placed at an angle of 20 degrees from vertical in the right lateral orbitofrontal cortex (LO) at coordinates anterior-posterior (AP) +4.2mm, medial-lateral (ML) -2.2 mm, superior-inferior (SI) -4.2 mm. For seizure initiation and local field potential (LFP) recording, twisted pair bipolar electrodes with tips separated by 1mm, insulation shaved distally to 0.3 mm, and electrode tips in the coronal plane were implanted into the dorsal hippocampus at (HC) at coordinates AP -3.8, ML 2.5, SI -3.2 mm. Additionally, a stainless steel anchoring screw (0-80 x 3/32; PlasticsOne, Roanoke, VA) was placed caudal to the hippocampal electrode and was affixed to this electrode with acrylic dental cement (Lang Dental Manufacturing, Wheeling, IL; powder: REF 1220, jet liquid: REF 1403) for stability. MUA recordings were accomplished by placement of monopolar tungsten microelectrodes in coordinates corresponding to their nuclei. For ANT, these were AP -1.4 mm, ML 1.5 mm, SI -5.6 mm. For CL, these were AP -2.8 mm, ML 1.5 mm, SI -5.2 mm. For VPM, these were AP -3.3 mm, ML 2.4 mm, SI -6.2 mm.

Juxtacellular recordings from CL were accomplished by placement of a glass electrode placed at the same coordinates as above with a micromanipulator (AP -2.8

mm, ML 1.5 mm, SI -5.2 mm) similar to procedures described elsewhere (7, 14-16). Borosilicate glass capillaries (#1B150F-4, World Precision Instruments) measuring 1.5 mm by 100 mm were pulled on a Flaming/Brown micropipette puller (Sutter Instruments, P-1000 horizontal puller), and then bumped under microscopy to form a flat electrode tip. These capillaries were then filled with with 4% Neurobiotin (Vector Laboratories, SP-1120) in saline (0.9% NaCl).

Seizure initiation

The protocol for this model of limbic seizure initiation has been described previously (17). Seizures were initiated several hours after the completion of electrode implantation, to allow time for the animal to come out of deep anesthesia. Light anesthesia status was assessed by the presence of less than 3 slow waves on LO LFP every 10 seconds, while the animal was still unresponsive to toe pinch stimulation. Seizures were then triggered by a 2 second 60Hz biphasic square pulse of variable current from a stimulator (A-M Systems, Model 2100). The current was manually selected to elicit a seizure of at least 30 seconds (assessed based on polyspike hippocampal MUA) and did not secondarily generalize. This latter criterium was assessed by polyspike activity in the LO LFP, and any seizures that did generalize were excluded from analysis. The current required to trigger an appropriate seizure varied from 100 – 900 μA. Currents at smaller amplitudes tended to be insufficient, and at larger amplitudes tended to generalize.

Signal acquisition and recording

MUA sampling electrodes were connected to amplifiers (A-M Systems, Model 1800). Their signals were recorded with 1000x amplifier gain, and then high pass filtered at 400-10,000 Hz on an analog filter (Model 3364; Krohn-Hite). They were then digitized on a Power 1401 (CED) at a sampling rate of 20 kHz to ensure sufficient resolution. These data were then imported to Spike2 (CED) software for analysis (see below).

Similar to above, LFP signals from LO were recorded at 1000x amplifier gain on a microelectrode amplifier (A-M Systems, Model 1800), but were filtered at 0.1 – 100 Hz on an analog filter (Model 3364; Krohn-Hite). The signals were then digitized on a Power 1401 (CED) at a sampling rate of 1 kHz to minimize file size. These data were then imported to Spike2 (CED) software for analysis (see below).

SUA signals from placed electrodes were acquired with an Axoclamp-2B amplifier (Molecular Devices, x10 gain, current clamp mode). These signals were digitized at 20,000 Hz with a Power 1401 and Spike2 software (as above, both from CED). Once a neuron signal was stably recorded during the baseline, ictal, postictal, and recovery epochs, it would be labeled by passing current pulses (0.6–10 nA, pulse duration 150 ms, 3 Hz) through the electrode tip to eject the Neurobiotin, for later

placement confirmation with histology. These current pulses were driven for > 15 min to improve labelling.

Histology

Animals were perfused transcardially with 0.2% heparinized phosphate-buffered saline (PBS) (APP Pharmaceuticals, Lake Zurich, IL) followed by 4% paraformaldehyde (PFA) (JT Baker, Center Valley, PA) in PBS. The brain was then removed and post-fixed for at least 12 hours in 4% PFA in PBS at 4 C. Brains were washed three times in PBS in preparation for slicing, placed in 2% agarose gel (American Bioanalytical, Natick, MA) and cut at 60 µm on a Vibratome (Leica Microsystems, Wetzlar, Germany). MUA electrode placement was confirmed by the electrode track after staining with cresyl violet (FD NeuroTechnologies, Columbia, MD).

Juxtacellular electrode placement was confirmed by nickel stain. Brain sections were incubated for 10 min in 0.7% hydrogen peroxide in cold PBS, and then in biotinylated peroxidase (1:200, “B” component of standard ABC [avidin-biotin peroxidase complex] kit, Vector Laboratories) overnight. Using 3-3'-diaminobenzidine tetrahydrochloride (DAB) as a chromogen, the neuron was then intensified with nickel (Ni) by incubating the sections in a solution containing 0.05% DAB and 0.038% nickel ammonium sulfate for 5 minutes and then adding hydrogen peroxide to a final concentration of 0.01%, and agitating for an additional 5 minutes. The slices were then

rinsed thoroughly to remove any excess Ni-DAB not in the neuron of interest. The slices were then mounted on polarized slides (ThermoScientific, Waltham, MA, U.S.A.) and dried for at least 48 hours. In order to stain other brain structures, the slices were then stained with Cresyl Violet as above. Coverslips (Fisher Chemicals, Pittsburg, PA) were applied. Images of slices at 60x and 250x were taken on a compound light microscope (Carl Zeiss) with a digital camera (Motic), and digitally stitched together (Microsoft Image Composite Editor). Ni-DAB stained neurons were identified their black-deep brown color. Neuron locations in the CL were confirmed when they fell no more than 1.5 mm ventral to the hippocampus, and were just lateral to the stria medullaris/lateral habenula complex or the mediodorsal thalamic nucleus.

Statistics and Data Analysis

All data were analyzed in Spike2 (CED) and Excel (Microsoft, Redmond, WA). For MUA, spindle power, and LFP delta power analysis, analysis epochs were defined as follows: The baseline epoch was the 10 seconds prior to seizure onset, the ictal period was the first 30 seconds of seizure activity (defined by polyspike discharges from on the hippocampal LFP electrode), the post-ictal epoch was defined as the 10 seconds following seizure offset, and the recovery epoch was defined as the last 10 seconds before the animal was re-anesthetized or the experiment terminated. Neuronal firing was assessed in MUA through analysis of root mean square voltage (Vrms), as validated in epilepsy models elsewhere as matching neuronal firing based on spike sorting (9, 17,

18). This was used in ANT, CL, and VPM recordings, in consecutive overlapping one second time bins.

Spindle waves were analyzed by downsampling the MUA from 20 kHz (as above) to 100 Hz, which resulted in an amplitude profile corresponding to the 7-14 Hz spindle activity and removed most background 7-14 Hz LFP signal. With this amplitude profile, we then measured power in the downsampled MUA using 2.56 second overlapping bins to obtain "spindle power". In addition to thalamic nuclei, we also assessed cortical activity by recording LO local field potential (LFP) during limbic seizures. Using Spike2 (CED) we calculated delta (0-4 Hz) power in 1 second overlapping time bins.

To show a time course of mean percent changes for MUA Vrms, "spindle power" and delta power, we plotted [(ictal signal - mean baseline)/mean baseline] x 100%, for consecutive 1 second nonoverlapping intervals. We then calculated the mean percent changes for each epoch. Although it may be intuitive to average across all seizures, this approach is subject to outlier animals if it has many seizures. The alternative, averaging within each animal first, is subject to outliers with few seizures. While we performed both analyses, the figures shown here were performed after averaging within each animal first, as this approach generates a smaller sample size and is more conservative.

Repeated-measures analysis of variance (ANOVA) was used to detect electrophysiological changes in CL, ANT, VPM, and LO by contrasting values in the

preseizure baseline with ictal, postictal, and recovery epochs. All statistical tests were performed using SPSS 17 (IBM), and significance level was set at $p < 0.05$.

SUA was spike sorted using Spike2, and single units were identified with template matching. Using an in-house MATLAB (R2009a, The MathWorks) program, we generated and analyzed Raster plots of neuron firing and burst firing over the different time epochs (baseline, ictal, and postictal, as above). Histograms of mean firing rate were calculated in 1 second overlapping bins for each epoch. Only data from electrodes whose correct locations were confirmed on histology were analyzed.

Interspike interval (ISI) analysis

For analysis of SUA, we looked at the ISI in the ictal period versus baseline. ISI is defined as the time in milliseconds between sequential peaks in action potentials (19). These measurements were exported to MATLAB (R2009a, The MathWorks), where we generated logarithmic histograms of the data. For a qualitative assessment of the change in firing rate, we compared the fraction of action potentials that occurred in tonic versus burst firing patterns using χ^2 analysis. As established in prior studies, we defined burst firing as ≥ 2 consecutive action potentials with an ISI ≤ 10 milliseconds (20).

Results

LO LFP Activity during seizures

The use of monitoring LFP in LO has been well established for monitoring of cortical activity in this model of temporal lobe epilepsy (17, 21). In this study, we used these recordings to correlate simultaneous activity in the cortex with the thalamic nuclei of interest. LFP during seizures in the cortex shows stereotypical large amplitude slow waves, which we quantified by measuring delta-band power (0 – 4 Hz) in each of the epochs. As has been previously shown, delta power significantly ($p < 0.05$) increased in LO during ictal and postical epochs, and returned to baseline levels in the recovery epoch (Figure 1).

ANT MUA recordings demonstrate trend of increased Vrms during limbic seizures

ANT is a complex and fascinating structure. Anatomically, it rests that the superior region of the thalamus, segmented off from the rest of the structure by the anterior internal medullary lamina. It is divided into 3 subdivisions, anteroventral, anterodorsal, and anteromedial (5). ANT has connectivity to the hippocampus, the anterior and posterior cingulate cortices, and the retrosplenal cortex, amongst others. Physiologically, its role in the limbic system makes it a significant player in circuits involved in episodic memory and arousal.

Pathologically, it is implicated in limbic seizure propagation and maintenance. As such, it has been considered a promising target for deep brain stimulation in the treatment of medically refractory epilepsy (22, 23). Most notably, stimulation of this nucleus was explored in the recent SANTE trial for drug-resistant epilepsy (24). The SANTE trial was an RCT which targeted ANT with DBS in patients with medically uncontrolled epilepsy. Over the course of 4 months, patients who received DBS demonstrated a 25% decrease in seizure reduction rate over controls. Subjects did have some notable side effects (notably some memory impairment), and the device has not approved by the FDA (25).

As a critical player in the limbic system previously implicated in epilepsy, we would expect significant changes in ANT during limbic seizures. We performed measurements of MUA activity in ANT over the course of 31 distinct focal limbic seizures in 10 different animals (Figure 2). We found that ANT neurons tended to show ictal increased firing, but this trend did not meet significance ($p < 0.05$) (Figure 3).

While this finding was not significant when all seizures were examined, the majority of animals (8/10) demonstrated a significant increase in MUA Vrms during seizures. This increase was not significant when data were first pooled with each animal, nor was it significant when seizures were pooled across animals. Figure 4 shows electrode locations within ANT after cresyl violet staining for each experiment.

MUA Vrms decreases in CL during limbic seizures

The intralaminar thalamus has long been recognized as a key player in arousal and awareness as an important relay in the ascending reticular activating system between the brainstem and cortex (26). Clinically, stimulation of this region has been correlated with increased arousal in humans (27), in addition to attention and goal-seeking behavior(26). Recent studies have elucidated the role of this region in decreased arousal during seizures, and have narrowed our focus to a specific nucleus within it: the centrolateral nucleus (7, 28).

We performed measurements of MUA in CL over the course of 30 distinct focal limbic seizures in 9 different animals (Figure 5). Ictally, MUA Vrms was found to be significantly decreased on average ($p < 0.05$, Figure 6). Figure 7 confirms electrode locations within CL after cresyl violet staining.

Juxtacellular recordings in CL show a decreased firing rate and a shift from tonic to burst firing

We conducted juxtacellular recordings to more precisely assess the behavior of neurons in CL in 8 animals, assessing the activity of 12 neurons during 14 seizures. Our MUA recordings had shown decreased activity in the structure, but these recordings do not show the firing rate or pattern of individual neurons. We found that the neurons in

CL had a significantly decreased firing frequency during seizures. The baseline firing rates varied between neurons, but 11/12 neurons examined showed a decreased firing rate during seizures. The average firing rate decreased by a statistically significant ($p < 0.05$) 51.87 ± 19.29% during the ictal epoch compared to preictal baseline (Figure 8A,B).

In addition to a decrease firing rate, we observed a change in firing pattern. Typically, in baseline epochs, these neurons would demonstrate a tonic firing pattern, defined as consecutive spikes with > 10 ms interval between them. During ictal and postical epochs, we observed a much greater proportion of firings in burst pattern (χ^2 = 634.1, 223.6, respectively, $p < 0.0001$). These neurons generally returned to baseline firing patterns in the recovery epoch (Figure 8C-E).

The location of each neuron was confirmed by sectioning the brain and staining with Ni-DAB and cresyl violet, as described above. The position of these electrodes are shown in Figure 9.

MUA Vrms and spindle power in VPM increase during limbic seizures

Physiologically, spindles are thought to play a role in both sensory processing and long term memory consolidation (29, 30). As they are most typically seen during states of decreased arousal, recording their presence during seizures could indicate if and how this pathway was interrupted in limbic epilepsy. Within the thalamus, spindles

are most typically seen in relay nuclei (31), such as VPM. VPM normally acts as a relay in for somatosensory afferents from the face, with projections to the postcentral gyrus and primary somatosensory cortex.

During 30 focal seizures in 11 rodents, MUA Vrms measurements in VPM showed a significant ($p < 0.05$) increase in MUA during seizures (Figure 10). In the same experiments, we also found a significant ($p < 0.05$) increase in spindle power ictally compared to baseline (Figure 11). Both spindle power and MUA returned to normal during the recovery epoch. Figure 12 shows electrode locations within VPM after cresyl violet staining.

Discussion

We found varying activity in our investigation of neuronal activity in ANT, CL, and VPM during focal limbic seizures. While CL demonstrated decreased ictal population firing on MUA measurements, both ANT and VPM showed increased ictal population firing relative to baseline. Examination of spindle waves within VPM showed a sharp increase in frequency. Finally, SUA within CL showed a decrease in firing rate and an increase in burst firing during seizures. While results in ANT did not reach statistical significance ($p < 0.05$), the results do generally support the hypothesis that different thalamic nuclei play significantly different roles in focal limbic seizures.

These last findings generally support the previous understanding of ANT in epilepsy. With its sophisticated connections to the hippocampus and mammillary bodies for memory, it is unsurprising that it plays a role in focal limbic epilepsy (32). Indeed, lesions to the anterior thalamus are associated with anterograde amnesia, suggesting a role as one of the primary outputs from the hippocampus in memory. Assuming hippocampal seizures are likewise transmitted to ANT, the increased MUA we recorded makes sense. Paralleling our recording from ANT, we observed increased LFP in HC during seizures, with decreased potential in the postictal epoch. This supports a model for seizure propagation from the hippocampus and to the cortex via ANT. This could suggest that stimulation in ANT serves a disruptive function which interrupts this

pathway, limiting focal limbic seizures, and explaining the therapeutic attributes of this stimulation in epilepsy.

While CL's role in epilepsy is less well established than ANT, it has a role in arousal that is becoming increasingly clear (26). In animals, increased activity of this nucleus has been tied to visuomotor stimuli (33, 34). In human experiments, intralaminar stimulation has been successful in improving certain cognitively mediated behaviors in a patient with severe traumatic brain injury (27) and in producing behavioral and electrographic arousals from spontaneous sleep (35).

While no experiments with CL stimulation have been performed in humans with epilepsy, stimulation of other intralaminar nuclei have shown promise in rodents. Bilateral high-frequency CL stimulation improved postictal electrophysiology after focal limbic seizures, demonstrating decreased cortical slow waves and increased desynchronization (28). Perhaps most exciting during that study was a resumption of baseline exploratory behavior in the postictal state. Further progress was made when bilateral CL stimulation was combined with bilateral stimulation of the pontine nucleus oralis, a structure in the pontine reticular formation, which has previously been shown to promote wake-like electrophysiology when stimulated (36, 37). With this paradigm, stimulated rodents showed behavioral arousal during seizures, resuming apparently physiologic exploratory behavior (38). Our findings of decreased ictal MUA activity support previous understanding of the nucleus's importance in promoting arousal.

The SUA recordings from CL demonstrated a shift from tonic solitary spikes at baseline and converting to burst firing ictally. These two patterns of firing are physiologically observed in many thalamic relay cells, and reflect the varying voltage-dependent transmembrane conductance (39). There are subtle, but significant, differences in the processing of inputs during each of the firing patterns, allowing for a degree of signal filtering and promoting at the thalamic level. Some thalamic nuclei, notably in the lateral geniculate nuclei, typically fire tonically, but respond to visual stimuli more vigorously when switching to burst mode. Similarly, cells in the thalamic have been observed to enter burst mode when entering slow wave sleep or deep anesthesia in animals (10).

While our findings do not prove that the switch to burst firing during limbic seizures is responsible for loss of consciousness, these findings do support a model that places the decreased arousal in limbic seizures in the same paradigm as that seen in anesthesia or slow wave sleep. Furthermore, the putative roles of CL as part of a larger model does suggest that its activity may contribute to decreased cortical activity during seizures. This model, the network inhibition hypothesis, states that suppression of subcortical structures, including the upper brainstem reticular formation and intralaminar thalamic nuclei, is fundamental to loss of consciousness in focal limbic epilepsy (40, 41).

Our recordings of MUA in VPM correlated well with LFP in LO. Both showed ictal and postictal increases in Vrms and delta power respectively, which returned to baseline levels in the recovery epochs. Moreover, the increase in cortical slow waves in LO was accompanied by increased spindle power in ictal and postical epochs. Spindle waves are a well described finding in thalamocortical networks during slow wave sleep, sensory processing, and generalized seizures. They typically appear as 7-14 Hz oscillations that increase and decrease in amplitude every 2-4 seconds (42). They are thought to be generated in the thalamus and more specifically the thalamic reticular and relay nuclei (31). Interestingly, this receives significant cholinergic input from the pedunculopontine tegmental nucleus, a major component of the reticular activating system (43). Much of the support for the network inhibition hypothesis stems from observations that subcortical cholinergic suppression is involved in decreased arousal during the ictal and postictal phases of focal temporal lobe seizures (7, 44, 45). It is possible that the suppression of cholinergic afferents to VPM, in addition to the thalamic reticular nucleus, contributes to the formation of sleep spindles, as observed in this study.

While we have gained significant insight into the behavior of these nuclei, there are many questions that remain unanswered. Further studies could expand our results into other areas of the brain. Our study placed significant stress on the interplay between these nuclei and other subcortical structures implicated in arousal, notably the thalamic reticular nucleus. Additionally, findings from incidental neurostimulation to

this area during seizures has suggested that stimulation of the thalamic reticular nucleus, like other CL and the pontine nucleus oralis, may help restore arousal during seizures. An assessment of its behavior during seizures could be insightful as to its role towards both arousal and sleep spindle formation. Similar studies could also be performed in pontine nuclei as well, as suspected components of subcortical arousal circuitry.

One additional limitation was the use of anesthesia. The cocktail we used was mild, but could have altered the underlying neurophysiology. Other studies using less invasive techniques (EEG and imaging) have been accomplished without anesthesia, but these do not approach the accuracy of intracranial, direct measurements. Rodent models of temporal lobe epilepsy have been used successfully in experiments without anesthesia (38), and we have some measurements of MUA from these. No studies have done juxtacellular readings in unanesthatized animals, and this does present a logistical and technical challenge to future investigators.

This study provides precise measurements of several thalamic nuclei during focal limbic seizures. These nuclei, ANT, CL, and VPM, showed different activity, reflecting different roles in seizure pathology. The recordings, when placed in the greater context of other studies, allow us to postulate that some of these locations are involved in seizure propagation, while others are involved in suppression of arousal. While future studies will have to further clarify the sophisticated pathways underlying epilepsy, this is

a significant step in promoting our understanding. And with greater understanding, we may develop novel therapeutics or interventions to lessen the burden of those with epilepsy.

Bibliography

1. Yuen AWC, Thompson PJ, Flugel D, Bell GS, and Sander JW. Mortality and morbidity rates are increased in people with epilepsy: Is stress part of the equation? *Epilepsy & Behavior.* 2007;10(1):1-7.
2. Sadler RM. The syndrome of mesial temporal lobe epilepsy with hippocampal sclerosis: clinical features and differential diagnosis. *Adv Neurol.* 2006;97(27-37.
3. Blumenfeld H. What is a seizure network? Long-range network consequences of focal seizures. *Adv Exp Med Biol.* 2014;813(63-70.
4. He X, Doucet GE, Sperling M, Sharan A, and Tracy JI. Reduced thalamocortical functional connectivity in temporal lobe epilepsy. *Epilepsia.* 2015;56(10):1571-9.
5. Child ND, and Benarroch EE. Anterior nucleus of the thalamus: functional organization and clinical implications. *Neurology.* 2013;81(21):1869-76.
6. Mueller SG, Laxer KD, Barakos J, Cheong I, Finlay D, Garcia P, Cardenas-Nicolson V, and Weiner MW. Involvement of the thalamocortical network in TLE with and without mesiotemporal sclerosis. *Epilepsia.* 2010;51(8):1436-45.
7. Motelow JE, Li W, Zhan Q, Mishra AM, Sachdev RN, Liu G, Gummadavelli A, Zayyad Z, Lee HS, Chu V, et al. Decreased subcortical cholinergic arousal in focal seizures. *Neuron.* 2015;85(3):561-72.
8. Mishra AM, Ellens DJ, Schridde U, Motelow JE, Purcaro MJ, DeSalvo MN, Enev M, Sanganahalli BG, Hyder F, and Blumenfeld H. Where fMRI and electrophysiology agree to disagree: corticothalamic and striatal activity patterns in the WAG/Rij rat. *J Neurosci.* 2011;31(42):15053-64.
9. Schridde U, Khubchandani M, Motelow JE, Sanganahalli BG, Hyder F, and Blumenfeld H. Negative BOLD with large increases in neuronal activity. *Cereb Cortex.* 2008;18(8):1814-27.
10. Steriade M, McCormick D, and Sejnowski T. Thalamocortical oscillations in the sleeping and aroused brain. *Science.* 1993;262(5134):679-85.
11. Mejias-Aponte CA, Jimenez-Rivera CA, and Segarra AC. Sex differences in models of temporal lobe epilepsy: role of testosterone. *Brain Res.* 2002;944(1-2):210-8.
12. Janszky J, Schulz R, Janszky I, and Ebner A. Medial temporal lobe epilepsy: gender differences. *J Neurol Neurosurg Psychiatry.* 2004;75(5):773-5.
13. Paxinos G. In: Watson C ed. San Diego :: Academic Press; 1998.
14. Duque A, and Zaborszky L. *Neuroanatomical Tract-Tracing 3*. Springer; 2006:197-236.
15. Pinault D. A novel single-cell staining procedure performed in vivo under electrophysiological control: morpho-functional features of juxtacellularly labeled thalamic cells and other central neurons with biocytin or Neurobiotin. *J Neurosci Methods.* 1996;65(2):113-36.

16. Zhan Q, Buchanan GF, Motelow JE, Andrews J, Vitkovskiy P, Chen WC, Serout F, Gummadavelli A, Kundishora A, Furman M, et al. Impaired Serotonergic Brainstem Function during and after Seizures. *J Neurosci.* 2016;36(9):2711-22.

17. Englot DJ, Mishra AM, Mansuripur PK, Herman P, Hyder F, and Blumenfeld H. Remote effects of focal hippocampal seizures on the rat neocortex. *J Neurosci.* 2008;28(36):9066-81.

18. Shmuel A, Augath M, Oeltermann A, and Logothetis NK. Negative functional MRI response correlates with decreases in neuronal activity in monkey visual area V1. *Nat Neurosci.* 2006;9(4):569-77.

19. Chen L, Deng Y, Luo W, Wang Z, and Zeng S. Detection of bursts in neuronal spike trains by the mean inter-spike interval method. *Progress in Natural Science.* 2009;19(2):229-35.

20. Kros L, Eelkman Rooda OHJ, Spanke JK, Alva P, van Dongen MN, Karapatis A, Tolner EA, Strydis C, Davey N, Winkelman BHJ, et al. Cerebellar output controls generalized spike‐and‐wave discharge occurrence. *Annals of Neurology.* 2015;77(6):1027-49.

21. Englot DJ, Yang L, Hamid H, Danielson N, Bai X, Marfeo A, Yu L, Gordon A, Purcaro MJ, Motelow JE, et al. Impaired consciousness in temporal lobe seizures: role of cortical slow activity. *Brain.* 2010;133(12):3764-77.

22. Hodaie M, Wennberg RA, Dostrovsky JO, and Lozano AM. Chronic anterior thalamus stimulation for intractable epilepsy. *Epilepsia.* 2002;43(6):603-8.

23. Samadani U, and Baltuch GH. Anterior thalamic nucleus stimulation for epilepsy. *Acta Neurochir Suppl.* 2007;97(Pt 2):343-6.

24. Fisher R, Salanova V, Witt T, Worth R, Henry T, Gross R, Oommen K, Osorio I, Nazzaro J, Labar D, et al. Electrical stimulation of the anterior nucleus of thalamus for treatment of refractory epilepsy. *Epilepsia.* 2010;51(5):899-908.

25. Dalkilic EB. Neurostimulation Devices Used in Treatment of Epilepsy. *Curr Treat Options Neurol.* 2017;19(2):7.

26. Van der Werf YD, Witter MP, and Groenewegen HJ. The intralaminar and midline nuclei of the thalamus. Anatomical and functional evidence for participation in processes of arousal and awareness. *Brain Research Reviews.* 2002;39(2):107-40.

27. Schiff ND, Giacino JT, Kalmar K, Victor JD, Baker K, Gerber M, Fritz B, Eisenberg B, Biondi T, O'Connor J, et al. Behavioural improvements with thalamic stimulation after severe traumatic brain injury. *Nature.* 2007;448(7153):600-3.

28. Gummadavelli A, Motelow JE, Smith N, Zhan Q, Schiff ND, and Blumenfeld H. Thalamic stimulation to improve level of consciousness after seizures: evaluation of electrophysiology and behavior. *Epilepsia.* 2015;56(1):114-24.

29. Andrillon T, Nir Y, Staba RJ, Ferrarelli F, Cirelli C, Tononi G, and Fried I. Sleep spindles in humans: insights from intracranial EEG and unit recordings. *The Journal of Neuroscience.* 2011;31(49):17821-34.

30. Holz J, Piosczyk H, Feige B, Spiegelhalder KAI, Baglioni C, Riemann D, and Nissen C. EEG sigma and slow-wave activity during NREM sleep correlate with overnight declarative and procedural memory consolidation. *Journal of Sleep Research.* 2012;21(6):612-9.

31. Steriade M, and Deschenes M. The thalamus as a neuronal oscillator. *Brain Research Reviews.* 1984;8(1):1-63.

32. Aggleton JP, O'Mara SM, Vann SD, Wright NF, Tsanov M, and Erichsen JT. Hippocampal-anterior thalamic pathways for memory: uncovering a network of direct and indirect actions. *Eur J Neurosci.* 2010;31(12):2292-307.

33. Schlag J, and Schlag-Rey M. Visuomotor functions of central thalamus in monkey. II. Unit activity related to visual events, targeting, and fixation. *Journal of Neurophysiology.* 1984;51(6):1175-95.

34. Hunsperger RW, and Roman D. The integrative role of the intralaminar system of the thalamus in visual orientation and perception in the cat. *Experimental Brain Research.* 1976;25(3):231-46.

35. Westmoreland BF, Groover RV, and Klass DW. Spontaneous sleep and induced arousal. A depth-electroencephalographic study. *J Neurol Sci.* 1976;28(3):353-60.

36. Morison R, Dempsey E, and Morison B. Cortical responses from electrical stimulation of the brain stem. *American Journal of Physiology--Legacy Content.* 1940;131(3):732-43.

37. Moruzzi G, and Magoun HW. Brain stem reticular formation and activation of the EEG. *Electroencephalogr Clin Neurophysiol.* 1949;1(4):455-73.

38. Kundishora AJ, Gummadavelli A, Ma C, Liu M, McCafferty C, Schiff ND, Willie JT, Gross RE, Gerrard J, and Blumenfeld H. Restoring Conscious Arousal During Focal Limbic Seizures with Deep Brain Stimulation. *Cereb Cortex.* 2017;27(3):1964-75.

39. Sherman SM. Tonic and burst firing: dual modes of thalamocortical relay. *Trends Neurosci.* 2001;24(2):122-6.

40. Blumenfeld H. Impaired consciousness in epilepsy. *Lancet Neurol.* 2012;11(9):814-26.

41. Norden AD, and Blumenfeld H. The role of subcortical structures in human epilepsy. *Epilepsy Behav.* 2002;3(3):219-31.

42. von Krosigk M, Bal T, and McCormick D. Cellular mechanisms of a synchronized oscillation in the thalamus. *Science.* 1993;261(5119):361-4.

43. Hallanger AE, Levey AI, Lee HJ, Rye DB, and Wainer BH. The origins of cholinergic and other subcortical afferents to the thalamus in the rat. *The Journal of Comparative Neurology.* 1987;262(1):105-24.

44. Furman M, Zhan Q, McCafferty C, Lerner BA, Motelow JE, Meng J, Ma C, Buchanan GF, Witten IB, Deisseroth K, et al. Optogenetic stimulation of cholinergic brainstem neurons during focal limbic seizures: Effects on cortical physiology. *Epilepsia.* 2015;56(12):e198-202.

45. Li W, Motelow JE, Zhan Q, Hu YC, Kim R, Chen WC, and Blumenfeld H. Cortical network switching: possible role of the lateral septum and cholinergic arousal. *Brain Stimul.* 2015;8(1):36-41.

Figures

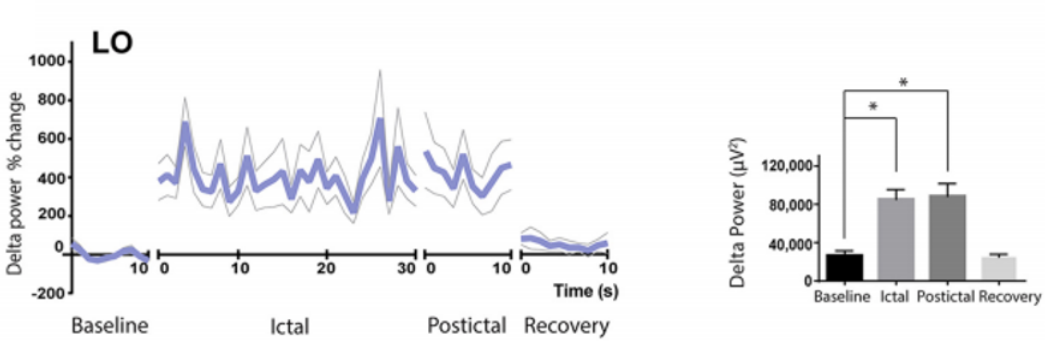

Figure 1: Change of delta power in various time epochs in LO

Delta-band power (0 -4 Hz) power is increased in LO in the ictal and postictal epochs, compared to baseline. It returns to baseline in the recovery epoch. Plot on left shows mean ± SEM at each time point, using 1 second bins. Histogram at right plots mean delta power at each epoch with error bars indicating SEM. ANOVA revealed significant differences between epochs, indicated by an asterisk. Data from 91 seizures in 30 animals. Reproduced from Feng et al., 2017.

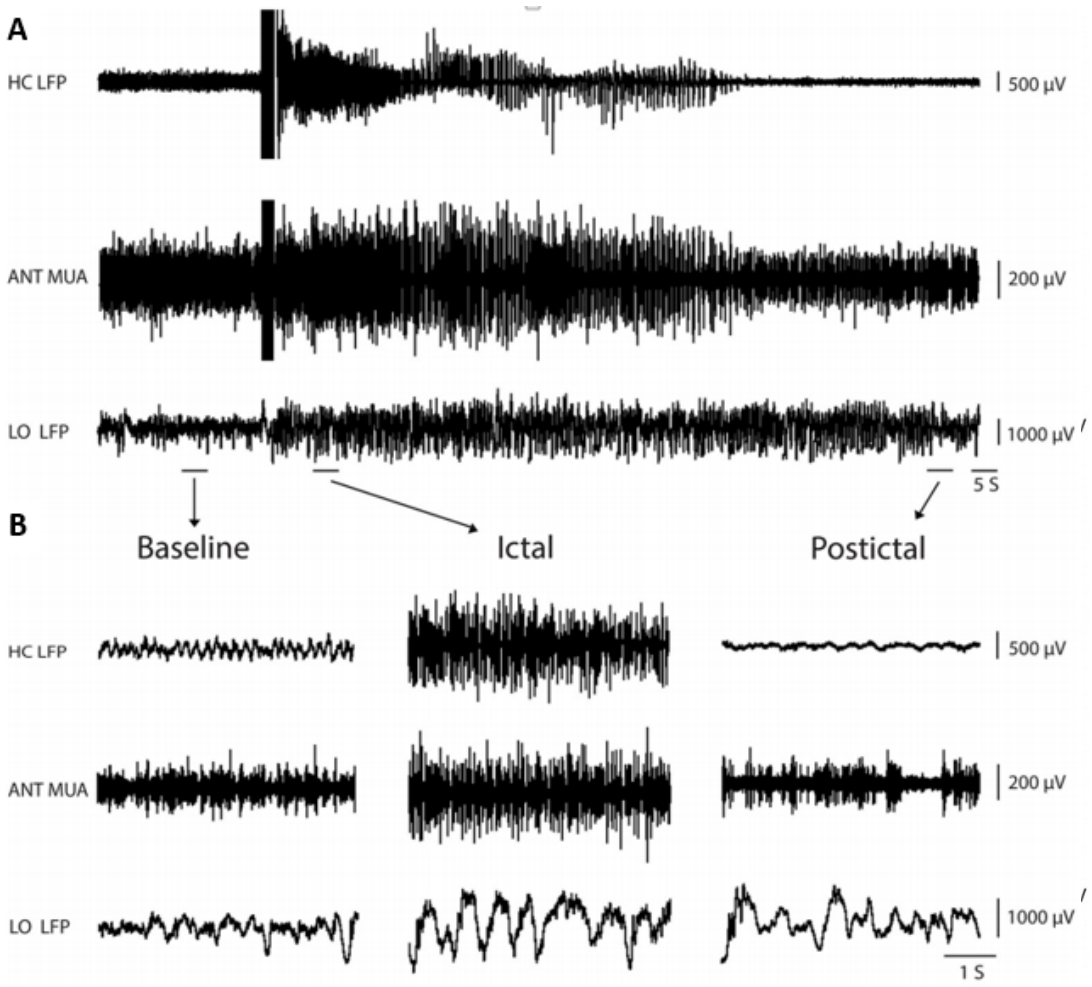

Figure 2: A representative example of MUA recordings in ANT during a seizure

(A) Recordings of HC LFP, ANT MUA, and LO LFP during baseline, ictal, and postictal epochs. Note the solid spike corresponding to the 2 second HC stimulus. (**B)**: 5 second samples of the aforementioned three epochs selected from the highlighted region and expanded over time. Note the increase in ANT MUA amplitude between baseline and ictal periods, and the subsequent decrease in the postictal period. This roughly correlates with LFP recordings from HC, which also showed increased activity ictally with postictal suppression. Reproduced from Feng et al., 2017.

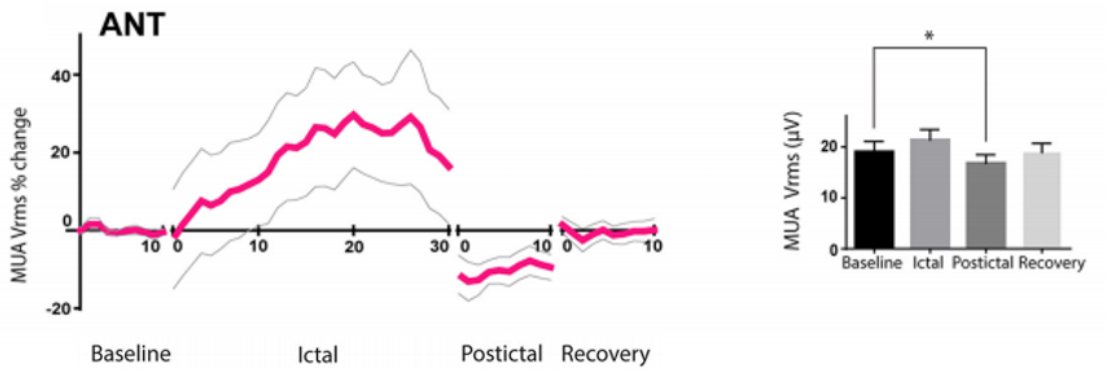

Figure 3: MUA Vrms in ANT

MUA increased in the ictal and decreased in the postical periods, compared to baseline, although the former did not reach statistical significance ($p < 0.05$). Plot on left shows mean ± SEM at each time point, using 1 second bins. Histogram at right plots mean MUA Vrms at each epoch with error bars indicating SEM. ANOVA revealed significant differences between epochs, indicated by an asterisk. Data from 31 seizures in 10 animals. Reproduced from Feng et al., 2017.

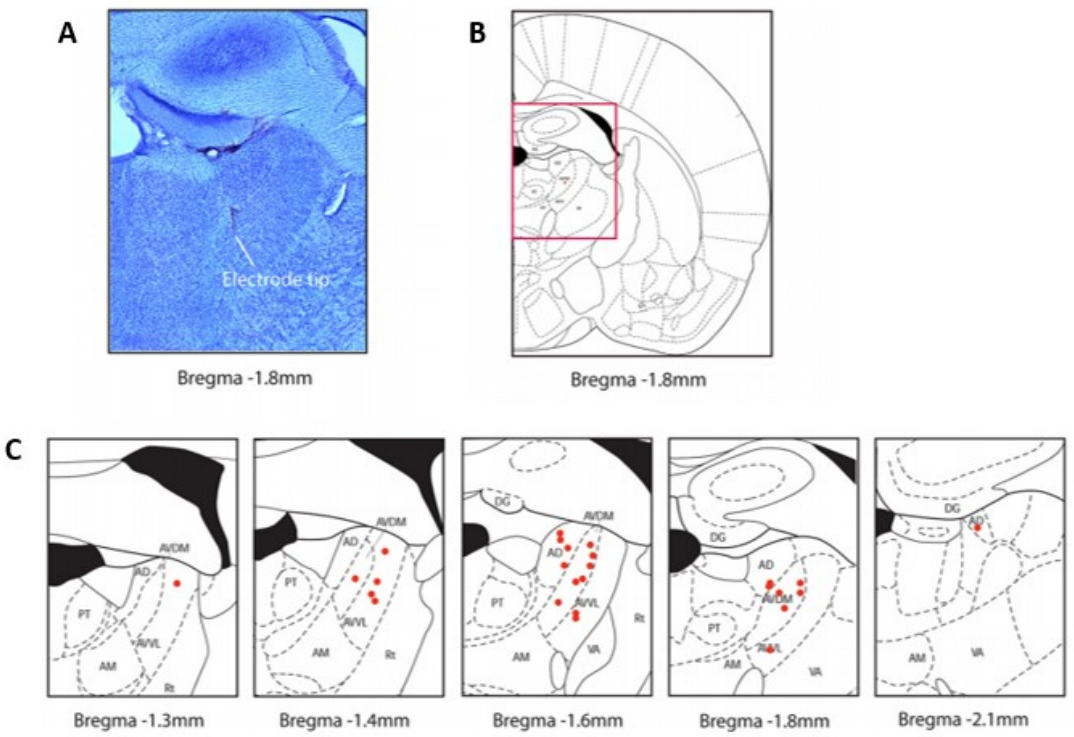

Figure 4: Histology showing location of MUA electrodes in ANT

(A) Representative example of brain slice post staining demonstrating electrode track and position of tip. **(B)** Map of rat brain at AP -1.8 mm from bregma with area corresponding to A outlined in pink. **(C)** Locations of electrode tips from rodents shown in red, confirming position in ANT. AM, Anteromedial nucleus of thalamus; AD, anterodorsal nucleus of thalamus; AVDM, anteroventral nucleus of thalamus, dorsomedial part; AVVL, anteroventral nucleus of thalamus, ventrolateral part; PT, paratenial nucleus of thalamus; Rt, reticular nucleus of thalamus; VA, ventral ANT; DG, dentate gyrus. Reproduced from Feng et al., 2017.

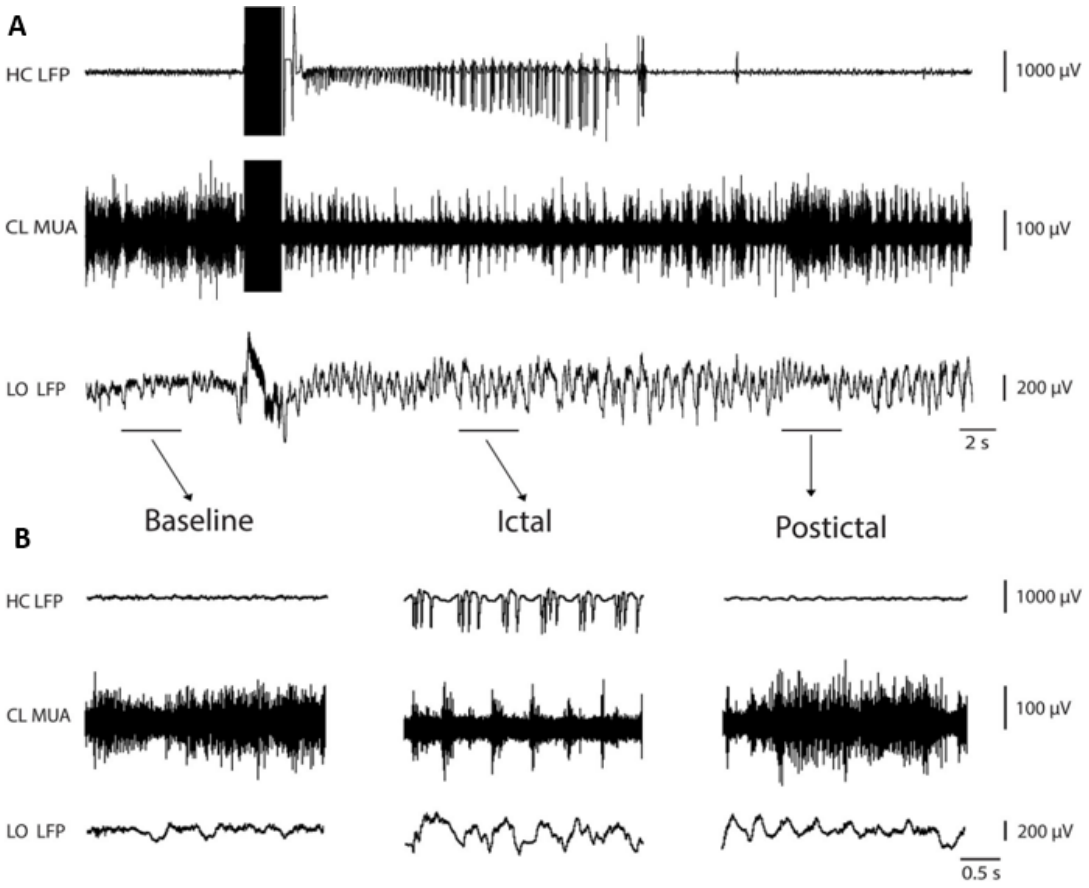

Figure 5: A representative example of MUA recordings in CL during a seizure

(A) Recordings of HC LFP, CL MUA, and LO LFP during baseline, ictal, and postictal epochs. Note the solid spike corresponding to the 2 second HC stimulus. **(B)** 5 second samples of the aforementioned three epochs selected from the highlighted region and expanded over time. Note the decrease in CL MUA amplitude between baseline and ictal periods. Reproduced from Feng et al., 2017.

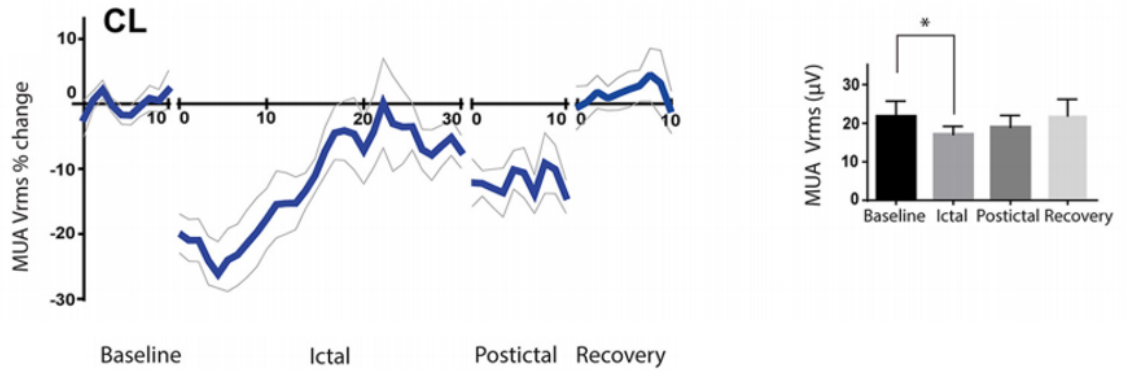

Figure 6: MUA Vrms in CL

MUA decreased in the ictal period, compared to baseline. This decrease gradually resolved during the postictal epoch, and was at baseline in the recovery epoch. Plot on left shows mean ± SEM at each time point, using 1 second bins. Histogram at right plots mean MUA Vrms at each epoch with error bars indicating SEM. ANOVA revealed significant differences between epochs, indicated by an asterisk. Data from 30 seizures in 9 animals. Reproduced from Feng et al., 2017.

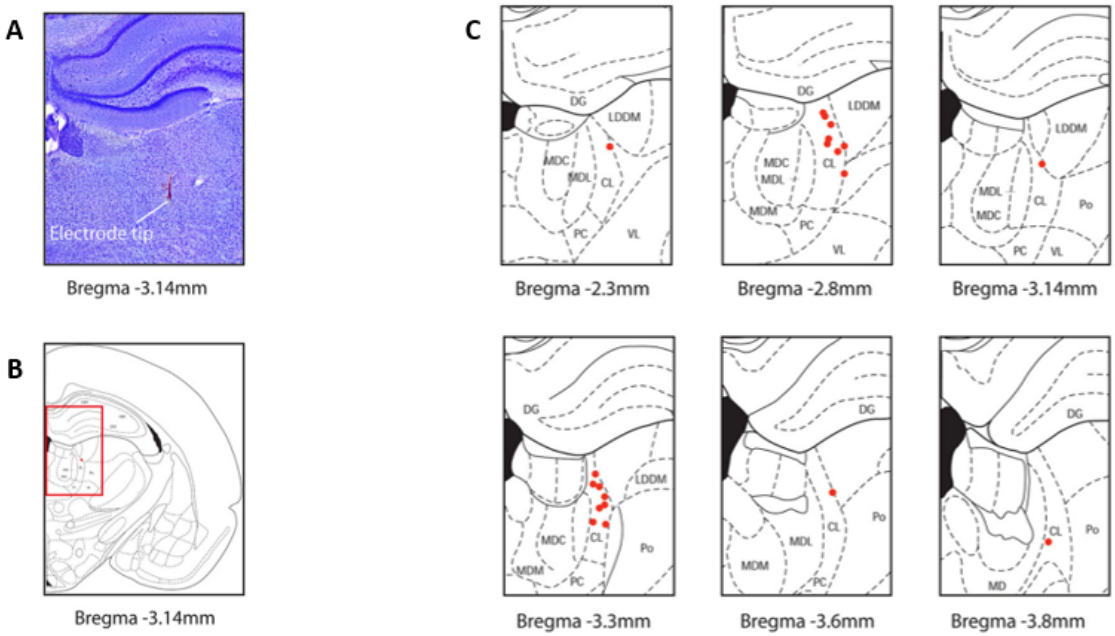

Figure 7: Histology confirming location of MUA electrodes in CL

(A) Representative example of brain slice post staining showing electrode track and position of tip. **(B)** Map of rat brain at AP -3.14 mm from bregma with area corresponding to A outlined in pink. **(C)** Locations of electrode tips from rodents shown in red, confirming position in CL. MD, Mediodorsal nucleus of thalamus; MDL, mediodorsal nucleus of thalamus, lateral part; MDM, mediodorsal nucleus of thalamus, medial part; MDC, mediodorsal nucleus of thalamus, central part; LDDM, laterodorsal nucleus of thalamus, dorsomedial part; PC, paracentral nucleus of thalamus; VL, ventrolateral nucleus of thalamus; Po, posterior nuclear group of thalamus; DG, dentate gyrus. Reproduced from Feng et al., 2017.

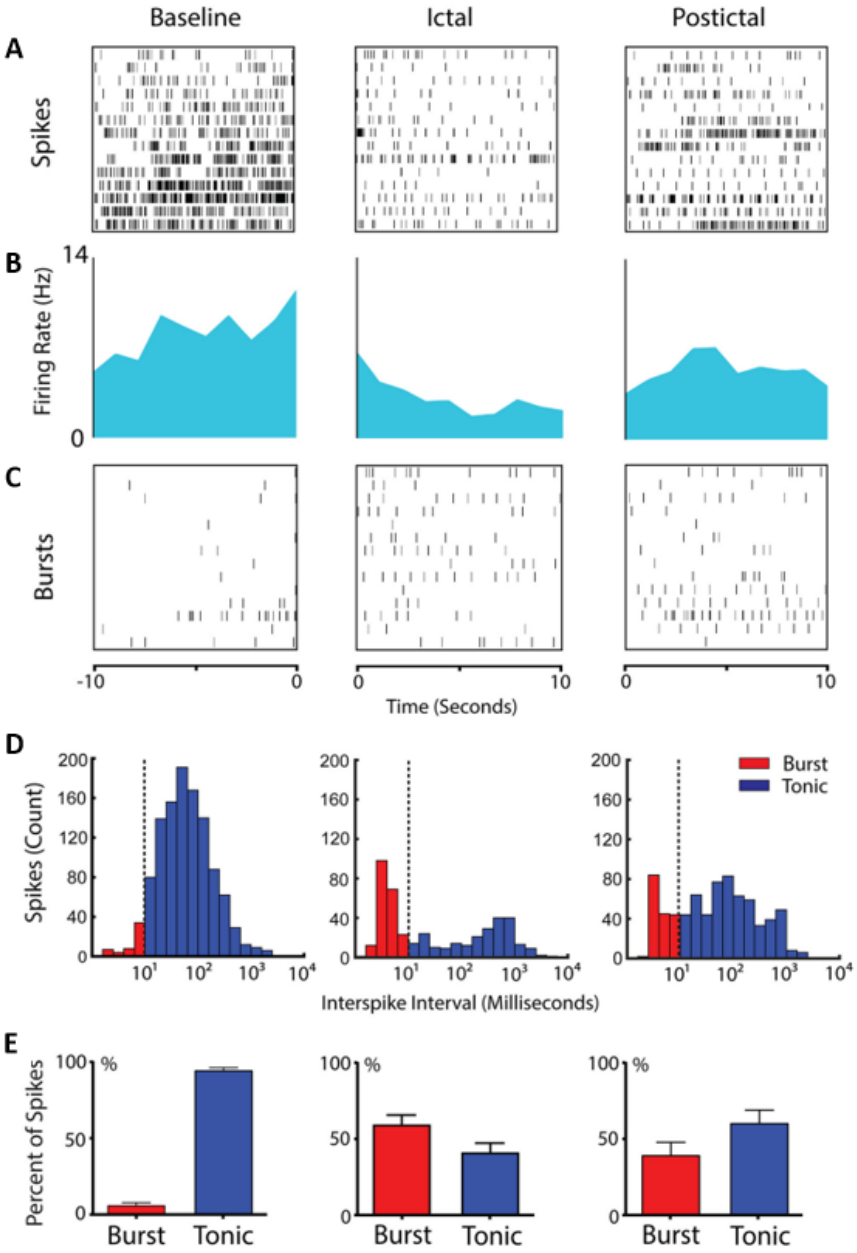

Figure 8: Neurons in CL show a decreased firing rate and increased burst firing during seizures

(A) Raster plot of all spikes in recorded neurons in labeled epochs. Each line indicates one spike. **(B)** Histogram of mean firing rates over time for each epoch. Data sorted into 1 second nonoverlapping bins. **(C)** Raster plot of each epoch with lines representing each burst. Each line represents a burst of at least 2 spikes. **(D)** Histogram of spikes

from Figure 8A sorted by length of ISI in milliseconds. Dashed line indicates 10 milliseconds, the cutoff between burst and tonic firing. **(E)** Comparison of the percentage of spikes falling into burst to tonic criteria in the different epochs. There was a dramatic increase in the proportion of neurons burst firing in the ictal and postical periods. **(A-E)** Data from 12 neurons during 14 seizures in 8 animals. Reproduced from Feng et al., 2017.

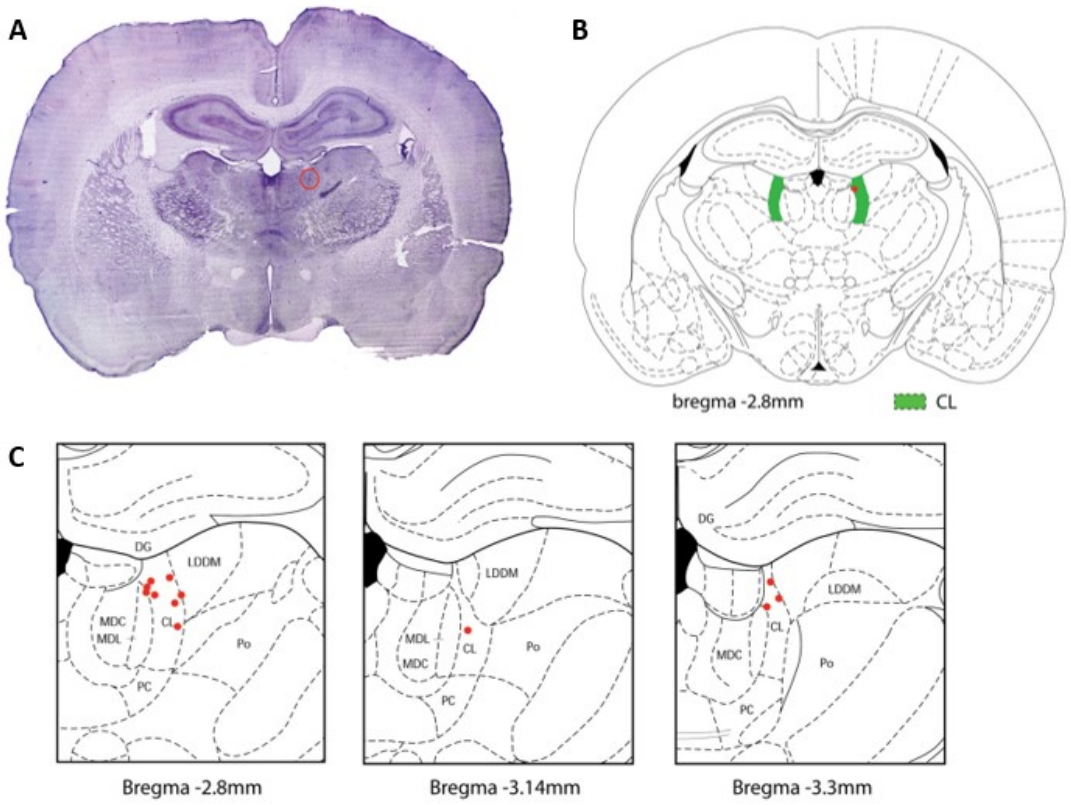

Figure 9: Histology confirming location of SUA electrodes in CL

(A) Representative example of brain slice post Ni-DAB and cresyl violet staining demonstrating position of stained neuron. **(B)** Map of rat brain at AP -2.8 mm from bregma with CL in green. **(C)** Locations of stained neurons from rodents shown in red, confirming position in CL. MDC, Mediodorsal nucleus of thalamus, central part; MDL, mediodorsal nucleus of thalamus, lateral part; LDDM, laterodorsal nucleus of thalamus, dorsomedial part; PC, paracentral nucleus of thalamus; Po, posterior nuclear group of thalamus; DG, dentate gyrus. Reproduced from Feng et al., 2017.

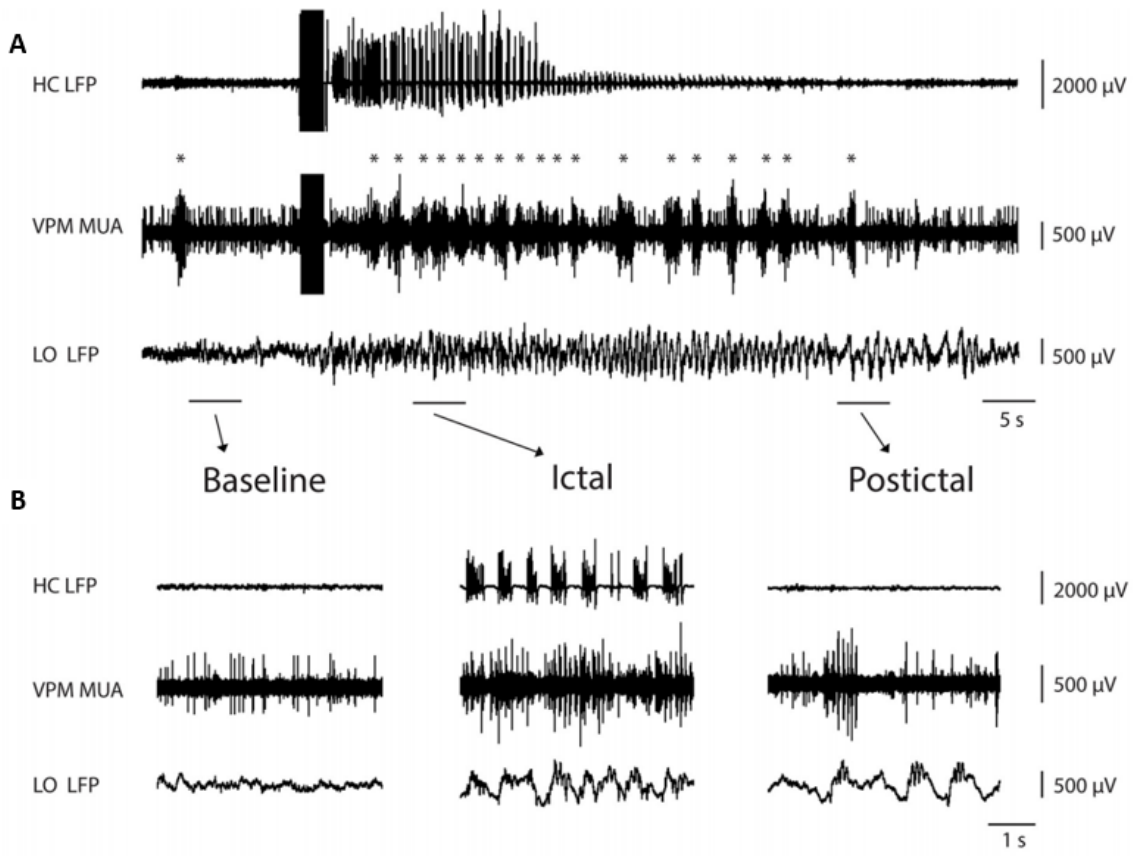

Figure 10: A representative example of MUA recordings in VPM during a seizure

(A) Recordings of HC LFP, VPM MUA, and LO LFP during baseline, ictal, and postictal epochs. Note the solid spike corresponding to the 2 second HC stimulus. Asterisks mark spindles. Ictally, spindle frequency increases dramatically, and returning to baseline in the postictal period. **(B)** 5 second samples of the aforementioned three epochs selected from the highlighted region and expanded over time. Note the increase in VPM MUA amplitude between baseline and ictal periods. Reproduced from Feng et al., 2017.

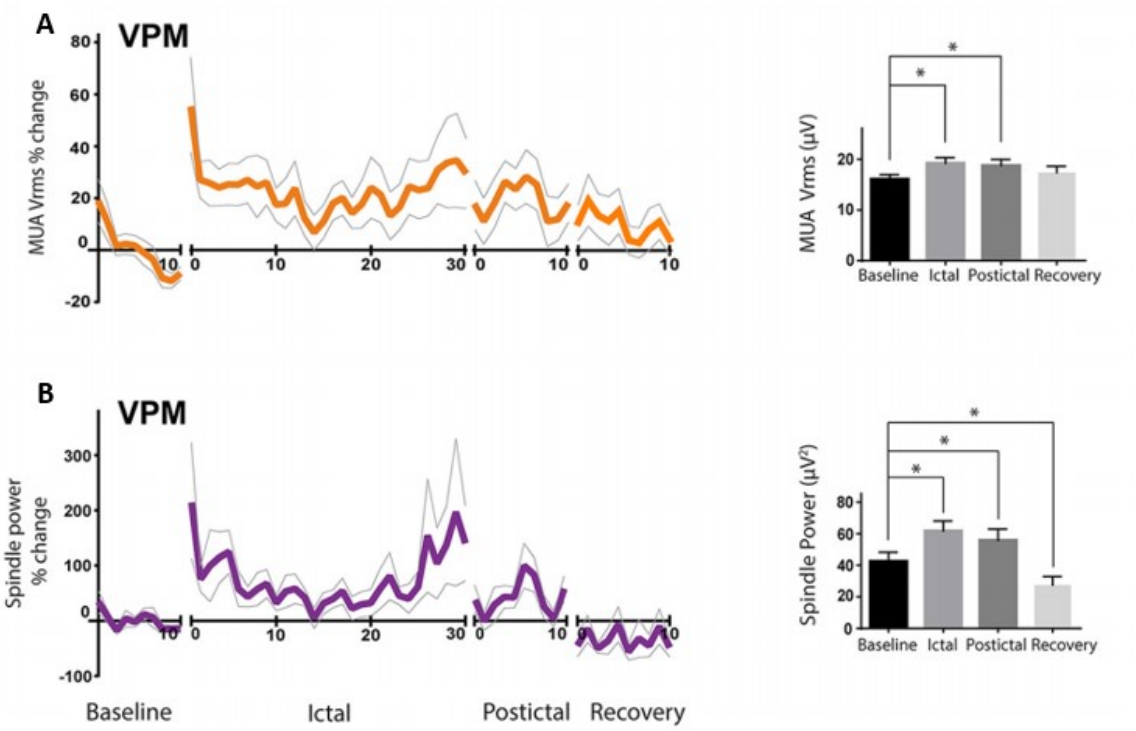

Figure 11: MUA Vrms and Spindle Power in VPM

(A) MUA Vrms increased in the ictal and postical periods on average, compared to baseline. **(B)** Spindle power (7-14 Hz) increased in the ictal and postictal periods, compared to baseline. In the recovery period however, there was a significant decrease in spindle power. **(A and B)** Plots on left show mean ± SEM at each time point, using 1 second bins. Histograms at right plot MUA Vrms and spindle power at each epoch with error bars indicating SEM. ANOVA revealed significant differences between epochs, indicated by an asterisk. Data from 30 seizures in 11 animals. Reproduced from Feng et al., 2017.

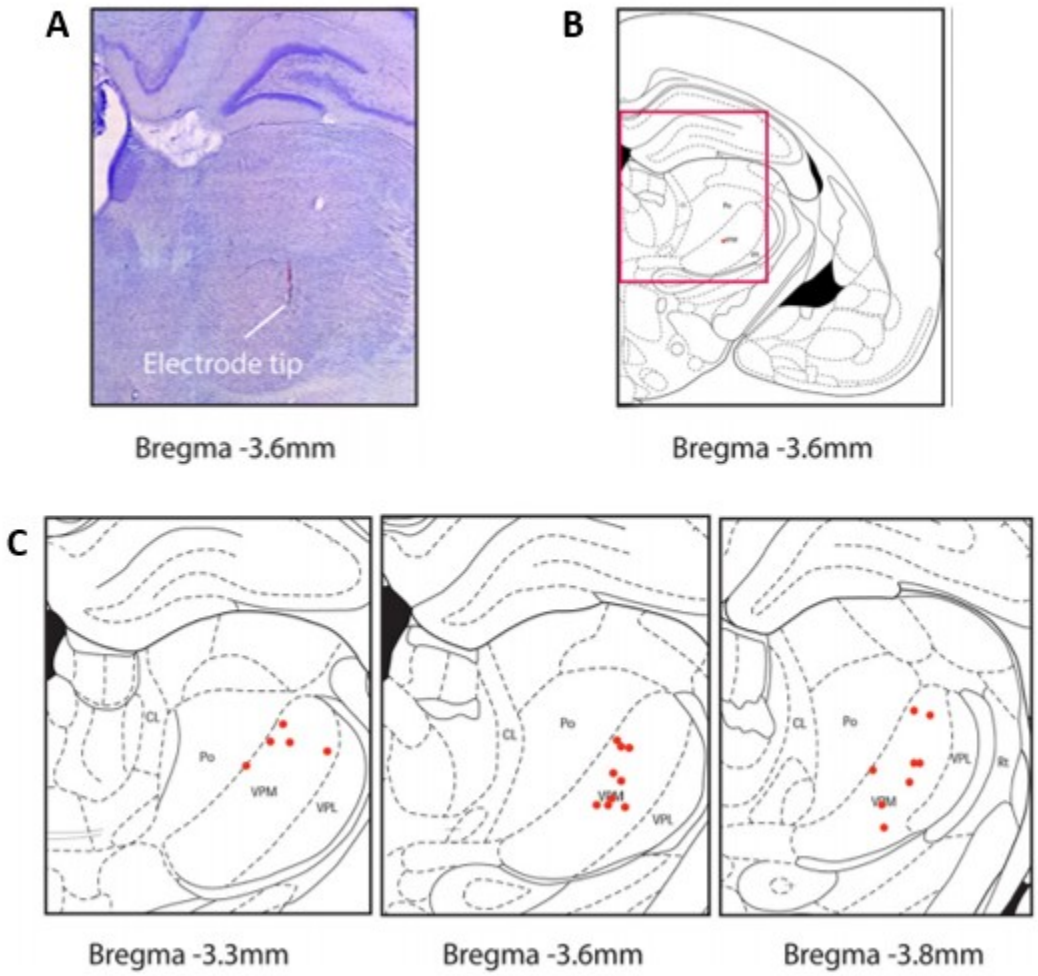

Figure 12: Histology confirming location of MUA electrodes in VPM

(A) Representative example of brain slice post staining demonstrating electrode track and position of tip. **(B)** Map of rat brain at AP -3.6 mm from bregma with area corresponding to A outlined in pink. **(C)** Locations of electrode tips from rodents shown in red, confirming position in VPM. AM, Anteromedial nucleus of thalamus; VPM, VPM nucleus of thalamus; CL, CL nucleus of thalamus; Po, posterior nuclear group of thalamus; VPL, ventral posterior lateral nucleus of thalamus; Rt, reticular nucleus of thalamus. Reproduced from Feng et al., 2017.